arXiv:1009.4682v1 [cond-mat.str-el] 23 Sep 2010

The origin of magnetic freezing in the pyrochlore $Y_2Mo_2O_7$

Oren Ofer,[1,2,*] Amit Keren,[2] Jason S. Gardner,[3,4] Yang Ren,[5] and W. A. MacFarlane[6]

[1] *TRIUMF, 4004 Wesbrook Mall, Vancouver, BC, V6T 2A3 Canada*
[2] *Department of Physics, Technion, Haifa 32000, Israel*
[3] *NCNR, National Institute of Standards and Technology, Gaithersburg, MD 20899-6102*
[4] *Indiana University, 2401 Milo B. Sampson Lane, Bloomington, IN 47408*
[5] *Advanced Photon Source, Argonne National Laboratory, 9700 South Cass Ave., Argonne, IL 60439 USA*
[6] *Department of Chemistry, University of British Columbia, Vancouver, BC, V6T 1Z1 Canada*

(Dated: February 23, 2024)

We investigated the nature of the spin glass-like phase transition in the geometrically frustrated pyrochlore lattices $Y_2Mo_2O_7$ using the local probes nuclear and muon magnetic resonances, and the field-dependent long range probes x-ray and neutron scattering. The long range probes indicated that $Y_2Mo_2O_7$ does not undergo any global symmetry changes, even in a field of 6 T. In contrast, the local signal indicates a lattice distortion close to the critical temperature. The nuclei show at least two inequivalent Y sites, and the muons show sub-linear line broadening as a function of moment size, over a wide temperature range. The conclusion from all the measurements is that even in high field, the distortion of $Y_2Mo_2O_7$ takes place within the unit-cell, while its global cubic symmetry is preserved. Moreover, the muon result clearly indicates the presence of magneto-elastic coupling.

PACS numbers: 75.50.Lk, 75.10.Nr

The Heisenberg model on the geometrically frustrated pyrochlore lattice has a macroscopically degenerate ground state, and the standard degeneracy-lifting mechanism of thermal or quantum fluctuation does not seem to remove it. Yet, with only one exception, the family of compounds based on $Tb_2Ti_2O_7$ [1–4], all pyrochlores freeze (at least partially), that is, one state out of many is selected. In some cases, like the spin ice, this is due to long-range interactions [5] and single ion anisotropy [6, 7]. In others, the freezing occurs even without anisotropy. In these cases magneto-elastic coupling might be responsible for the degeneracy lifting; the lattice distorts to relieve the frustrated interactions. Such a distortion might lead to a cubic-to-lower-symmetry structural transition [8]. This kind of frustration-driven distortion has been previously suggested as the main freezing mechanism for several $A_2B_2O_7$ pyrochlores [9, 10] and Cr spinels [11, 12], and was considered theoretically [13–16]. However, lattice distortions and symmetry changes as a function of temperature are a common feature in solids, even without magnetic interactions. Therefore, it is not yet clear whether: (I) the magnetic interactions drive the distortion; or (II) the distortion takes place because of electrostatic interactions, and the magnetic properties, such as freezing, follow. Clarification of this point is crucial for the understanding of the spin Hamiltonian, and therefore the ground state and excitations in pyrochlores. Field-dependence experiments can provide, in principle, answers to these questions.

One case is the pyrochlore $Y_2Mo_2O_7$ (YMO), which crystallize into a cubic structure with $Fd\bar{3}m$ symmetry [17]. Magnetically, it has a Curie-Weiss temperature of -200 K and freezes with spin-glass characteristics [18] at $T_f = 22.5$ K [19]. In particular, magnetization measurements indicate a large difference between zero-field-cooled and field-cooled magnetizations [20, 21]. This glassiness is unexpected if the chemical structure is perfect because it is believed that a spin-glass state emerges when frustration *and* disorder coexist. A possible solution to this dichotomy came from more detailed measurements. X-ray absorption fine structure spectroscopy

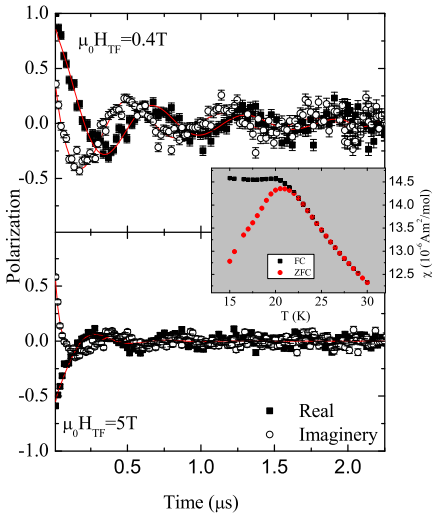


FIG. 1. (Color online) The raw muon depolarization data taken at $T = 24$K, at two transverse fields. The error bars represent statistical errors. The inset shows the bulk susceptibility $\chi = M/H$ versus temperature in zero-field cooled and field cooled conditions taken at a 1kG field.

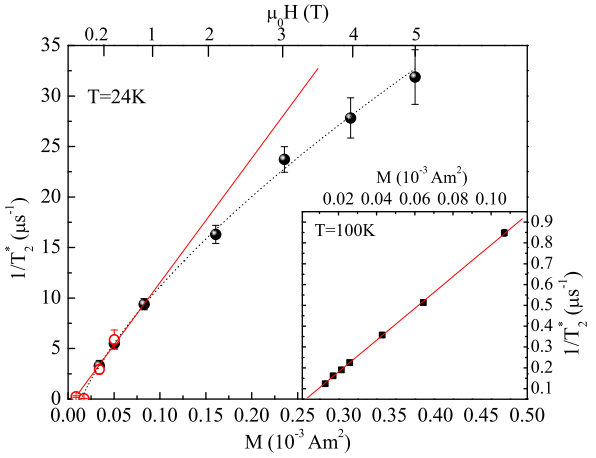


FIG. 2. (Color online) The TF-μSR relaxation rate, $1/T_2^*$, versus the magnetization, M at $T = 24$K. The field $\mu_0 H$ is an implicit parameter. Hollow circles are taken from Ref.[10]. The red (solid) line is a linear fit to low M data. The black (dotted) line is a fit to $A \cdot M^\beta$ where $\beta = 0.66(12)$. The inset shows $1/T_2^*$ versus M at $T = 100$ K.

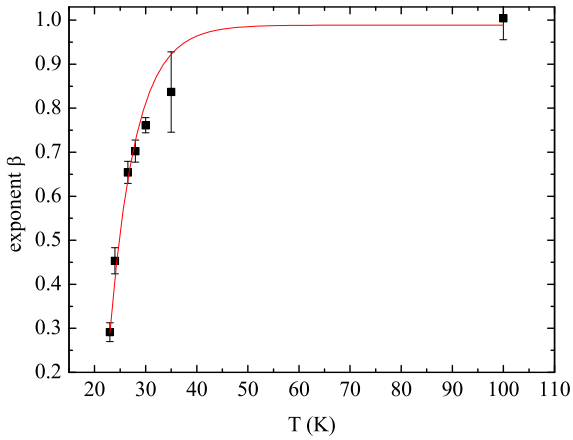


FIG. 3. (Color online) The exponent β versus the Temperature. β is extracted from $1/T_2^*$ versus the magnetization M fits to $1/T_2^* = AM^\beta$. Line is a guide to the eye.

(XAFS) in zero field show evidence of positional disorder of the Mo ion [22]. In contrast, neutron pair distribution function measurements assigned the distortion to the O1-Y bond [23]. Local magnetic probes, which are coupled to the spin system and operate in a field, such as ^{89}Y nuclear magnetic resonance (NMR) [9] and muon spin relaxation (μSR) [10], indicate a distortion of the spin-bearing ion, again the Mo. Despite the controversy on the distorted ion, all experiments suggest the lattice *is* taking part in the magnetic freezing. However, the presence of an applied field in the resonance measurements and its absence in scattering measurements make the comparison difficult. Moreover, neither experiment can shed light on the magneto-elastic coupling issue discussed above. The motivation of this work is to fill in the gap and perform both local resonance and long range scattering measurements under the same conditions, and to use the field as a probe of magneto-elastic coupling.

We performed five different experiments on YMO, which were carried out well above and close to T_f. (i) High transverse field (TF) and longitudinal field (LF) μSR, which extends previously low-field data [10, 24]. (ii) ^{89}Y NMR where we extend previous data [9] to the helium range. (iii) Field-dependent high resolution x-ray powder diffraction. (iv) Field-dependent neutrons diffraction, which extends the previous zero field (ZF) measurement [17, 23]. (v) Bulk magnetization using a superconducting quantum interference device (SQUID).

Polycrystalline samples of YMO were prepared according to Ref. [19]. The inset of Fig. 1 shows the zero-field-cooled (ZFC) and field-cooled (FC) magnetization measurements. The ZFC curve shows a distinctive maximum indicating the spin-glass transition. T_f and Curie-Weiss temperatures extracted from these measurements are in agreement with previous reports. In addition magnetization vs. applied field up to 5 T at various temperatures was also recorded and will be used below.

μSR measurements were performed at TRIUMF, Canada on the HiTime and Helios spectrometers in the M15 surface muon channel. Figure 1 depicts the raw muon polarization taken at a constant temperature, $T = 24$ K, at two transverse fields $\mu_0 H_{\rm TF} = 0.4$ and 5 T. The data is shown in a rotating-reference frame [25] of $\mu_0 H_{\rm RRF} = \mu_0 H_{\rm TF} - 0.02$ T. The TF relaxation rate increases with increasing fields. The LF (not shown) is at least an order of magnitude smaller than the TF relaxation rate at any field and temperature. This means the muon depolarization is mainly due to static field inhomogeneities and the contribution of the out-of-plane depolarization can be neglected. We found that the μSR TF asymmetry is best described by

$$P_{\rm TF}(t) = P_0 \exp\left(-\sqrt{t/T_2^*}\right) \cos(\omega t + \varphi) \qquad (1)$$

where P_0 is the initial polarization and $\omega = \gamma_\mu H_{\rm TF}$. The fits are represented by the solid line in Fig. 1.

In Fig. 2 we plot the transverse field relaxation rate $1/T_2^*$ at a given field versus the magnetization M measured at the same field, at temperature fixed at 24 K, slightly above the spin-glass freezing. We also show the field, H, as an explicit parameter on the upper abscissa. As the field increases the relaxation rate $1/T_2^*$ increases. However above $M = 10^{-4}$ Am^2, $1/T_2^*$ is no longer a linear function of M. This is not the case at higher temperatures. For comparison, in the inset of Fig. 2 we plot

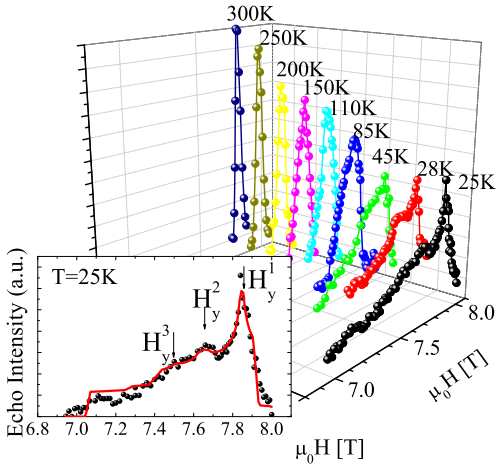


FIG. 4. (Color online) The NMR spectra at $25 \leq T \leq 300$ K. Inset: the NMR spectrum at $T = 25$ K. The line is a fit to a powder spectrum with three sites. The arrows point to the main peak in the powder spectrum of each site.

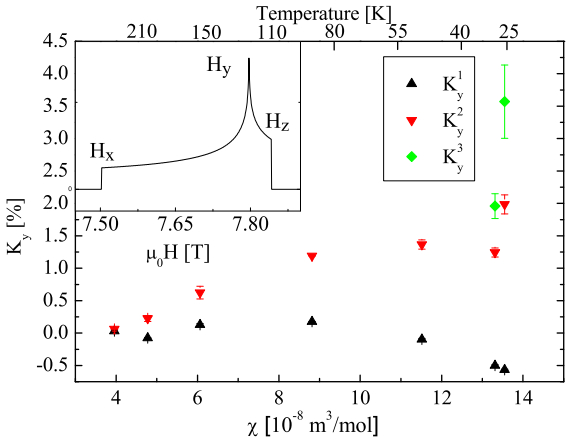


FIG. 5. (Color online) The NMR shift, K_y, versus the bulk susceptiblity χ and the temperature as an implicit parameter. In the inset, a theoretical powder spectrum of a nuclear spin 1/2 is depicted.

$1/T_2^*$ vs M taken at 100 K, again with H as an implicit parameter. At this temperature the relaxation rate is a linear function of M.

In a system with quenched disorder it is expected that $1/T_2^* \propto M$ [2, 26] as is indeed observed at 100 K. However, when T approaches T_f, the data deviates from this linearity and $1/T_2^*$ grows more slowly than M as depicted in Fig. 2. Fits to $1/T_2^* = AM^\beta$ are also shown in the figure, giving $\beta = 0.66(12)$ and $\beta = 1.00(2)$ for $T = 24$ and 100 K respectively. It is found that the transition from $\beta = 1$ to very low values are spread over a wide temperature range (Fig. 3).

One possibility is a site-dependent spin polarization due to impurities [27]. However, this can be ruled out by the undetectable amount of disorder in the sample. A more likely scenario is that the disorder in YMO is not quenched and at low T it varies with the field. In fact, the sub-linear behavior suggests that as the field (and M) increases the lattice is more ordered. This is the main finding of this work, which clearly points to the presence of a magneto-elastic coupling.

More evidence for temperature dependent disorder comes from ^{89}Y NMR which extends previous measurements [9] down to 25 K. Such low-T measurements were made possible by using a high pressure cell where higher RF power can be delivered to the sample. At each temperature we obtain the complete NMR spectrum by sweeping the external field, H_{ext}, at a constant applied RF frequency $f = 16.44$ MHz. In each field we used the spin-echo sequence ($\pi/2 - \pi$ pulses) and recorded the echo signal. In Fig. 4 we present the spectra taken at temperatures between 300 K and 25 K. The width of the 300 K spectrum extends over 0.1 T, whereas the width of the 25 K spectrum extends over 1 T. This broadening results in low intensities at each applied field upon cooling. Due to this broad line at low T we gave up on high resolution NMR, as in Ref. [9], and concentrated on the gross features of the spectrum. The most noticeable feature in the $T = 25$ K spectrum is the clear appearance of two peaks, with a hint of a third one. This suggests that out of the many different Y sites existing at high T[9], only few are being picked as T is lowered.

To understand this NMR spectrum we look at the spin 1/2 ^{89}Y nuclear spin Hamiltonian, which can be described as,

$$\mathcal{H} = -\hbar\gamma \mathbf{I} \cdot \left(\overline{\mathbf{1}} + \overline{\mathbf{K}}\right) \cdot \mathbf{H}_{ext} \qquad (2)$$

where $\overline{\mathbf{K}}$ is the NMR shift tensor, $\mathbf{I}$ is the nuclear spin operator, and $\mathbf{H}_{ext}$ is the variable applied field. In powders, the principal axes of $\overline{\mathbf{K}}$ are randomly oriented relative to $\mathbf{H}_{ext}$. Therefore, the magnetic resonance spectrum is an average over all possible orientations. A theoretical powder averaged NMR line [28], for a single site, is depicted in the inset of Fig. 5 where $H_\alpha = 2\pi f/[\gamma(1 + K_\alpha)]$ and $\alpha = x, y, z$ for the three directions. This theoretical spectrum demonstrates that a single site, with a single set of K_x, K_y, K_z, could give rise to only one peak even under powder averaging. The existence of two (perhaps three) peaks in the spectrum is a result of a lattice deformation leading to inequivalent Y sites.

In order to study the temperature dependence of the shift, we use the powder spectrum convoluted with Lorentzians to fit the NMR spectra. Such a fit is demonstrated by the solid line in the inset of Fig. 4. At high

temperatures ($T > 250$ K) the shift is very small; at intermediate temperatures, $50 \leq T \leq 200$ K, two different sites were needed to fit the data (see Fig. 4); and finally, at low enough temperatures, $T < 50$ K, three sites were assumed. In Fig. 5 we plot the shift K_y^i, i for each site, versus the bulk susceptibility, which was extrapolated to $\mu_0 H = 7.8$ T from the FC magnetization measurements. Temperature in this figure is an implicit parameter. As χ increases the shift for each site also increases. However, the dependence between shift and susceptibility is not linear. When the disorder is quenched one expects $K \propto \chi$. This proportionality is violated close to T_f, indicating that the lattice degrees of freedom are active as $T \to T_f$. It should be pointed out that unlike in μSR, in NMR it is impossible to vary the field over a wide range and NMR cannot be used to address the question of magneto-elastic coupling. In contrast, the presence of multiple sites well above T_f suggest that spin correlations are sufficient to distort the lattice.

We also searched for field effects in high resolution X-ray scattering. The X-ray powder diffraction experiments were conducted at the APS Argonne National Laboratory on the 11-ID-C beamline. A high-energy, 115 keV x-ray beam with a high-resolution analyzer was used with a 6 T magnet. In order to dismiss any grain orientation with the field, GE varnish was applied. In Fig. 6(a) we plot the most intense cubic (440) peak with and without an applied field at 60 K and 25 K. The peaks are field-independent in both shape and intensity. Needless to say, no peak splitting or new peaks were found when the field was applied and moreover the peaks are resolution limited. This rules out any global structural transition due to temperature or field.

Finally, similar experiments were performed using neutrons which are more sensitive to scattering from oxygen, but have lower resolution. These experiments were done on the BT1 powder diffractometer at NIST, Gaithersburg, USA, with a field up to 6 T perpendicular to the scattering plane. Data were collected at the same temperatures, with a neutron energy of $E = 34.5$ meV. In Fig. 6(b) we plot the (440) Bragg peak. As with the x-ray picture, no apparent difference is revealed between the measurements with and without the field. These peaks are resolution limited as well. However, the small difference in intensity at $T = 25$ K between the 6 T and zero field measurements is real and reproducible. It is probably due to very small structure-factor or magnetic form-factor changes induced by the field.

To conclude, both local probes unambiguously indicate a lattice deformation takes place as T approaches T_f. In addition, the magnetization dependence of the muon spin relaxation rate shows that lattice deformation is affected by magnetic field, therefore pointing to magneto-elastic coupling. Long range scattering measurements fail to detect global changes in the lattice parameters upon application of the field. Since the distortion is found locally

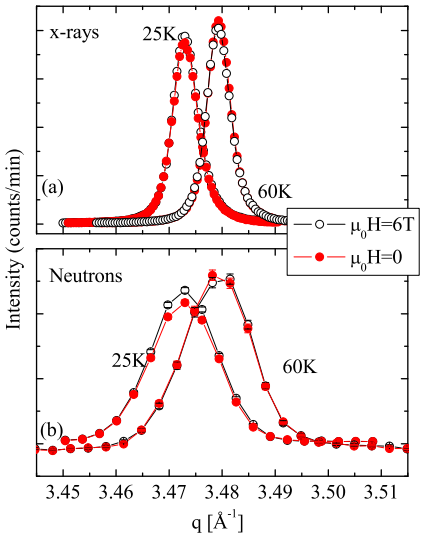


FIG. 6. (Color online) Field and temperature dependence of the (440) Bragg peak from (a) X-ray and (b) neutron scattering. The error bars representing statistical errors of $\pm 1\sigma$ are smaller than the symbols. The peaks in (a) and (b) are resolution limited.

by resonances, but not globally by scattering, it must be within the unit cell. It affects, at most, the structure-factors on the one hand, and the hyperfine coupling between Y nuclei and Mo spin on the other. Our work indicates that magneto-elastic coupling is part of the freezing process of YMO and provides a simple way to detect it in other magnets.

We are grateful to the staff of TRIUMF for assistance with the μ^+SR experiments. OO and AK acknowledge the financial support of NATO - Collaborative Linkage Grant, reference number PST.CLG.978705, the Israel-US Binational Science Foundation and the HFM network of the ESF, and the European Commission under the 6th Framework Programme through the Key Action: Strengthening the European Research Area, Research Infrastructures. Contract n°: RII3-CT-2004-506008. Use of APS was supported by the U.S. DOE under Contract No. DE-AC02-06CH11357.

* oren@triumf.ca

[1] J. S. Gardner, S. R. Dunsiger, B. D. Gaulin, M. J. P. Gingras, J. E. Greedan, R. F. Kiefl, M. D. Lumsden, W. A. MacFarlane, N. P. Raju, J. E. Sonier, I. Swainson and Z. Tun, Phys. Rev. Lett. **82** 1012 (1999).

[2] Oren Ofer, Amit Keren, Chris Baines and Jason S. Gardner , J. Phys.: Condens. Matter **19** 145270 (2007).

[3] I. Mirebeau, I. N. Goncharenko, P. Cadavez-Peres, S. T. Bramwell, M. J. P. Gingras and J. S. Gardner, Nature

420, 54 (2002).
[4] B. G. Ueland, J. S. Gardner, A. J. Williams, M.L. Dahlberg, J. G. Kim, Y. Qiu, J. R. D. Copley, P. Schiffer and R. J. Cava, Phys. Rev. B **81** 060408 (2010).
[5] Taras Yavors'kii, Tom Fennell, Michel J. P. Gingras, and Steven T. Bramwell, Phys. Rev. Lett. 101, 037204 (2008).
[6] S. T. Bramwell and Michel J. P. Gingras, Science **294** 1495 (2001).
[7] C. L. Henley, Phys. Rev. B **71** 014424 (2005).
[8] Y. Yamashita and K. Ueda, Phys. Rev. Lett. **85** 4960 (2000).
[9] Amit Keren and Jason S. Gardner, Phys. Rev. Lett. **87** 177201 (2001).
[10] Eva Sagi, Oren Ofer, and Amit Keren, Jason S. Gardner, Phys. Rev. Lett **94** 237202 (2005).
[11] S.-H. Lee, C. Broholm, T. H. Kim, W. Ratcliff II, and S-W. Cheong, Phys. Rev. Lett. **84** 3718 (2000).
[12] J-H. Chung, M. Matsuda, S.-H. Lee, K. Kakurai, H. Ueda, T. J. Sato, H. Takagi, K.-P. Hong, and S. Park, Phys. Rev. Lett **95** 247204 (2005).
[13] Oleg Tchernyshyov, R. Moessner, S. L. Sondhi, Phys. Rev. Lett. **88** 067203 (2002).
[14] D. L. Bergman, R. Shindou, G. A. Fiete, and L. Balents, Phys. Rev. B **74**, 134409 (2006).
[15] K. Penc, N. Shannon, and Hiroyuki Shiba, Phys. Rev. Lett. **93** 197203 (2004).
[16] T. E. Saunders and J. T. Chalker, Phys. Rev. Lett. **98**, 157201 (2007).
[17] J. N. Reimers and J. E. Greedan, and M. Sato, J. Solid State Chem. **72**, 390 (1988).
[18] M. J. P. Gingras, C. V. Stager, N. P. Raju, B. D. Gaulin, J. E. Greedan, Phys. Rev. Lett. **78**, 947 (1997).
[19] N. P. Raju, E. Gmelin, and R. K. Kremer, Phys. Rev. B, **46** 5405 (1992).
[20] K. Miyoshi, Y. Nishimura, K. Honda and J. Takeuchi, J. Phys. Soc. Japan. **69**, 3517 (2000).
[21] J. E. Greedan, M. Sato, Xu Yan and F. S. Razavi, Solid State Comm. **59**, 895 (1986).
[22] C. H. Booth, J. S. Gardner, G. H. Kwei, R. H. Heffner, F. Bridges, and M. A. Subramanian, Phys. Rev. B **62** R755 (2000).
[23] J. E. Greedan, Delphine Gout, A. D. Lozano-Gorrin, Shahab Derahkshan, Th. Proffen, H.-J. Kim, E. Bozin, and S. J. L. Billinge, Phys. Rev. B **79**, 014427 (2009).
[24] S. R. Dunsiger, R. F. Kiefl, K. H. Chow, B. D. Gaulin, M. J. P. Gingras, J. E. Greedan, A. Keren, K. Kojima, G. M. Luke, W. A. MacFarlane, N. P. Raju, J. E. Sonier, Y. J. Uemura, W. D. Wu, Phys. Rev. B. **54**, 9019 (1996).
[25] Tanya M. Riseman and Jess H. Brewer, Hyperfine Interactions **65**, 1107 (1990).
[26] P. Carretta and A. Keren, to appear in *Introduction to Frustrated Magnetism* edited by C. Lacroix, F. Mila, P. Mendels, (Springer, Berlin, 2011), In press.
[27] H. Alloul, J. Bobroff, M. Gabay, M. and P. J. Hirschfeld, Rev. Mod. Phys.**81** 45 (2009).
[28] P. C. Taylor, J. F. Baugher, and H. M. Kriz, Chem. Rev. **75** 203 (1975).